

Water vapor-assisted solid-state reaction for the synthesis of nanocrystalline BaZrO₃ powder

Takahiro KOZAWA,^{†,‡} Kazumichi YANAGISAWA* and Yoshikazu SUZUKI

Faculty of Pure and Applied Sciences, University of Tsukuba, 1-1-1 Tennodai, Tsukuba, Ibaraki 305-8573, Japan

*Research Laboratory of Hydrothermal Chemistry, Faculty of Science, Kochi University, 2-5-1 Akebono-cho, Kochi 780-8520, Japan

Solid-state reaction between BaCO₃ and ZrO₂ is the simplest method to prepare BaZrO₃, which is an important refractory structural material with a very high melting point and a low chemical reactivity. However, since the solid-state formation of the BaZrO₃ phase requires high calcination temperature, this method typically produces larger particles unsuitable for the sintering process than the solution methods. In this study, we investigated the reaction behavior between very fine ZrO₂ (70 nm) and coarse BaCO₃ (1.5–5.7 μm) and described the water vapor-assisted solid-state synthesis of BaZrO₃. Nanocrystalline BaZrO₃ powder (~80 nm) was obtained by solid-state reaction at 1050°C in air. The BaZrO₃ formation was accelerated by water vapor-assisted reaction. The apparent activation energy for the formation reaction was calculated to be 323 ± 21 kJ/mol and 263 ± 46 kJ/mol in air and humid air with H₂O of 0.5 atm, respectively. In the 1 atm water vapor atmosphere, almost single-phase BaZrO₃ was obtained by calcination at 750°C.

©2013 The Ceramic Society of Japan. All rights reserved.

Key-words : Barium zirconate, BaZrO₃, Nanocrystalline, Solid-state reaction, Water vapor, Water vapor-assisted reaction

[Received October 24, 2012; Accepted November 27, 2012]

1. Introduction

Among the synthetic methods for double-oxide powders, solid-state reaction between oxide and/or carbonate precursors is widely accepted as a simple and low-cost method. However, due to its relatively high calcination temperature, this method typically produces larger particles unsuitable for the sintering process than the solution methods.¹⁾ In order to overcome the high calcination temperature, a possible way is to reduce particle size of the raw materials. For example, one of the most important electroceramic materials, BaTiO₃, is prepared by the reaction between BaCO₃ and TiO₂ powders at about 1000°C. Recent studies have clearly shown that the reduction of particle size of BaCO₃ and TiO₂ results in a significant decrease of the temperature to complete the reaction.^{2)–5)} When the nanocrystalline powders are used in both raw materials, single-phase BaTiO₃ can be obtained at 700–800°C. Thus, the solid-state preparation using nanocrystalline raw materials is a promising alternative method to chemical routes for the synthesis of fine powders.

Barium zirconate, BaZrO₃, is an interesting refractory structural material with a very high melting point of 2690°C⁶⁾ and low chemical reactivity toward corrosive compounds like high temperature superconductors.^{7)–9)} Therefore, it is applied as crucible and substrate for the processing of these compounds. The fine BaZrO₃ powder is suitable for the fabrication of dense submicron ceramics.¹⁰⁾ In the powder synthesis of BaZrO₃ by solid-state reaction, Ubaldini et al.¹¹⁾ reported the preparation of nanocrystalline BaZrO₃ powder from very fine ZrO₂ (70–90 nm) and coarse BaCO₃ (~1 μm) powders. Interestingly, the final morphology of BaZrO₃ particles was determined by the initial

size and shape of original ZrO₂ particles. However, the formation reaction mainly occurred at 1000°C in dry air because of the requirement of thermal decomposition of coarse BaCO₃ particles. On the other hand, the reaction was accelerated in humid air with H₂O of only 0.02 atm than in dry air. It has been suggested that gas-phase transport of Ba(OH)₂, which is formed by the reaction of BaO with H₂O, to the surface of ZrO₂ particles proceeds under humid air and then the BaZrO₃ formation is accelerated. These results lead to the following strategies: in the solid-state synthesis of double-oxide powders, nanocrystalline powders can be prepared when the fundamental oxide powders are fine particles, though carbonates including the other constituting ions are larger particles. If the thermal decomposition of coarse carbonates is promoted, the formation reaction proceeds at a lower temperature than in air.

Recently, we have reported the water vapor-assisted solid-state reaction at 1 atm of H₂O for the formation of alkaline-earth titanates^{12),13)} and silicates.^{14),15)} Even though the relatively coarse raw materials were used, the solid-state reaction was dramatically accelerated by water vapor. The previous reports have clearly shown that water vapor promotes the decomposition of alkaline-earth carbonates. Thus, in the water vapor atmosphere, it is expected that the synthesis of nanocrystalline BaZrO₃ powder from very fine ZrO₂ and coarse BaCO₃ powders is achieved at a lower temperature.

In the present study, we describe the reaction behavior between very fine ZrO₂ and coarse BaCO₃ investigated by thermal analysis and in situ X-ray diffraction and the water vapor-assisted solid-state synthesis of BaZrO₃ under the different water vapor partial pressures.

2. Experimental

Elongated BaCO₃ particles ($S_{\text{BET}} = 1.68 \text{ m}^2/\text{g}$, length of 1.5–5.7 μm and aspect ratio of 3–5 from SEM observation) and nanocrystalline ZrO₂ powder (monoclinic phase, $S_{\text{BET}} = 14.1$

[†] Corresponding author: T. Kozawa; E-mail: t-kozawa@jwri.osaka-u.ac.jp

[‡] Present address: Joining and Welding Research Institute, Osaka University, 11-1 Mihogaoka, Ibaraki, Osaka 567-0047, Japan

m^2/g , $d_{\text{BET}} = 68 \text{ nm}$, $d_{50} = 70 \text{ nm}$) were used as raw materials. Nanocrystalline ZrO_2 powder was prepared by a crystallization of amorphous ZrO_2 , which was synthesized by a simple precipitation method from ZrOCl_2 and NH_3 .¹⁶⁾ The crystallization of amorphous ZrO_2 powder was conducted by calcination at 750°C for 2 h in air at a constant rate of $10^\circ\text{C}/\text{min}$. The amorphous phase was completely transformed to the monoclinic phase. All reagents were purchased from Wako Pure Chemical Industries, Ltd. Stoichiometric mixture of the reactants was prepared using wet mixing (ethanol, 2 h) by planetary ball milling (Fritsch, Pulverisette 6) with a zirconia pot and balls. After mixing, the slurry was dried at 80°C and finally sieved to be under $150 \mu\text{m}$.

Before calcination experiments, the reaction behavior of the mixture was investigated by thermogravimetric and differential thermal analysis (TG-DTA) and high-temperature X-ray diffraction (HT-XRD). TG-DTA experiment was performed at a constant heating rate of $5^\circ\text{C}/\text{min}$ in air (SII EXSTAR6300, Seiko). HT-XRD analysis was conducted by using an instrument of Multiflex ($\text{CuK}\alpha$, 40 kV, 40 mA, Rigaku Co.) in the range between room temperature and 1100°C in air. Each XRD pattern was acquired after 5 min holding at each temperature. The samples were mounted on a platinum plate and heated at a constant rate of $5^\circ\text{C}/\text{min}$.

The powder mixture placed in an alumina boat was calcined at various temperatures and times in air and water vapor by a tubular furnace. The calcination experiments in air were conducted in stagnant conditions. Those in water vapor were performed by flowing air at a flow rate of $500 \text{ mL}/\text{min}$, which was bubbled in a water bath. By adjusting the temperature of water bath, water vapor partial pressures were controlled between 0.1 and 0.5 atm. The humid air flow was introduced from $\sim 500^\circ\text{C}$. In the case of the 1 atm water vapor atmosphere, the tubular furnace equipped with a water evaporator was used. Distilled water was introduced at a flow rate of $1 \text{ mL}/\text{min}$ into the evaporator without a carrier gas from $\sim 500^\circ\text{C}$. Flow rate of water vapor was roughly estimated to be $\sim 1.3 \text{ L}/\text{min}$.

After calcination experiments, a powder XRD pattern of the sample at room temperature was recorded in the 2θ range between 10 and 70° with a 0.04° step and scanning speed of $4^\circ/\text{min}$. The reacted fraction (α) was defined as a ratio of the strongest XRD peak area of the BaZrO_3 against the total of that of each constituent phase. Specific surface area (S_{BET}) was measured by nitrogen adsorption isotherm analysis (BET method, Autosorb-3B, Quantachrome). The equivalent BET diameter (d_{BET}) was calculated from the following equation, $d_{\text{BET}} = 6/(\rho \cdot S_{\text{BET}})$, where ρ is the theoretical density. Particle size distribution was measured by laser diffraction-scattering particle size analyzer (SALD-7100, Shimadzu). The morphology of raw materials and calcined powders was characterized by field emission scanning electron microscopy (FE-SEM, JSM-6500F, JEOL) with Au coating.

3. Results and discussion

3.1 Reaction behavior of the BaCO_3 - ZrO_2 mixture

Figure 1 shows the DTG curve for the starting mixture corresponding to the first derivative of the weight loss curve. Two weight loss steps, which were located at 727 and 975°C , respectively, were observed. The weight loss in second step was much larger than that in the first step. The weight decrease behavior of the starting mixture was identical to that reported by Ubaldini et al.,¹¹⁾ because the particle size of raw materials was almost same. These weight loss steps caused by the decomposition of BaCO_3 may correspond to the formation of BaZrO_3 .

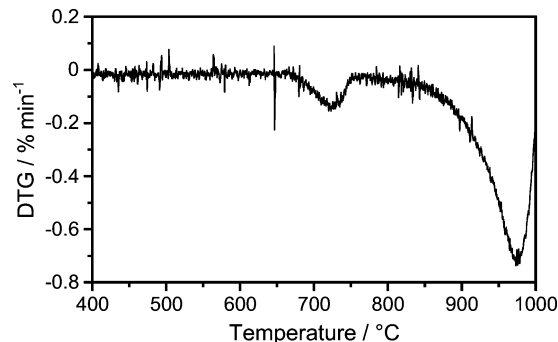


Fig. 1. DTG curve for the starting mixture recorded at $5^\circ\text{C}/\text{min}$ in air.

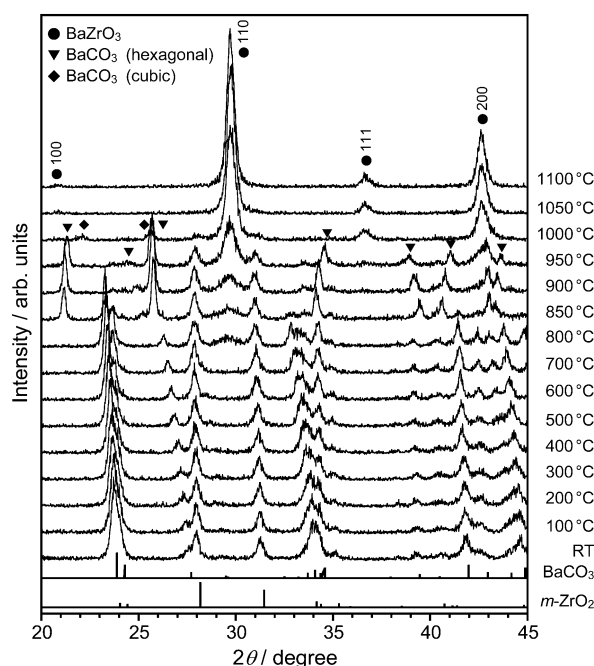


Fig. 2. HT-XRD patterns for the starting mixture recorded from room temperature to 1100°C in air. Standard XRD patterns of PDF No. 37-1484 for monoclinic ZrO_2 ($m\text{-ZrO}_2$) and PDF No. 45-1471 for orthorhombic BaCO_3 are also shown.

In situ XRD analysis was clearly indicated the formation behavior of BaZrO_3 during the heating. **Figure 2** shows the HT-XRD patterns for the starting mixture. The XRD pattern recorded at room temperature represented only orthorhombic BaCO_3 and monoclinic ZrO_2 phases. No phase change occurred up to 700°C . The XRD peaks of BaCO_3 were shifted to lower diffraction angles and split off with increasing temperature. These phenomena of the BaCO_3 phase are ascribed to the crystal thermal expansion and the formation of barium oxycarbonate with formula $\text{BaO}_x(\text{CO}_3)_{1-x}$, respectively.^{17,18)} The same results have been observed on the in situ investigation of the reaction between BaCO_3 and TiO_2 .¹⁹⁾ At 800°C , the (110) diffraction peak of BaZrO_3 slightly appeared. However, the peak intensity was the almost same up to 900°C . The BaZrO_3 formation occurred again from the heating at 950°C . The single-phase BaZrO_3 was obtained at 1050°C . The HT-XRD results indicate the formation steps of BaZrO_3 at 800 and 950°C and support the DTG results (Fig. 1). From these results, the first formation step involves a direct reaction between BaCO_3 and ZrO_2 , and the second forma-

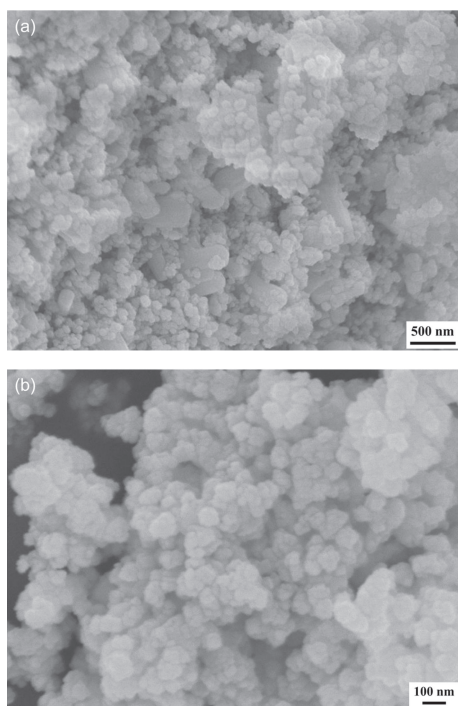


Fig. 3. SEM photographs of (a) the starting mixture and (b) the prepared BaZrO₃ powder at 1050°C for 2 h in air.

tion step at a higher temperature could also involve preliminary decomposition of BaCO₃, followed by a rapid reaction between BaO and ZrO₂.

The HT-XRD patterns also revealed that the orthorhombic-hexagonal and hexagonal-cubic phase transformations of BaCO₃ occurred at 850 and 1000°C, respectively. The temperature of these phase transformations has been reported to be 806 and 968°C in the pure BaCO₃, respectively.²⁰ On the other hand, the formation of BaO or other zirconium phases (Ba₂ZrO₄ and Ba₃Zr₂O₇)²¹ were not observed during the heating within the detection limit of XRD (~1 wt %).

Figure 3 shows the SEM photographs of starting mixture and BaZrO₃ powder obtained after calcination at 1050°C for 2 h in air. The elongated BaCO₃ particles with length of about 1 μm remained in the mixture and were covered with nanosized ZrO₂ particles [Fig. 3(a)]. The morphology of prepared BaZrO₃ particles was inherited from original ZrO₂ particles [Fig. 3(b)]. The BaZrO₃ powder consisted of primary particles with 70–80 nm. The S_{BET} of BaZrO₃ powders was 12.5 m²/g, and the d_{BET} was 77 nm. The primary particles shown in Fig. 3(b) were comparable with the equivalent particle size calculated from S_{BET} . Moreover, the size of BaZrO₃ particles was similar to the starting ZrO₂ particle size ($d_{\text{BET}} = 68$ nm).

3.2 Effect of water vapor on the solid-state synthesis

Water vapor accelerates the solid-state reaction for the preparation of BaZrO₃.¹¹ **Figure 4** shows the XRD patterns for the products obtained by calcination at 900°C for 2 h in air and humid air with various water vapor partial pressures. The peak intensities of BaCO₃ were decreased with increasing the water vapor partial pressure in the calcination atmosphere. Accordingly, the BaZrO₃ formation was accelerated by water vapor. By means of semi-quantitative analysis using integrated XRD intensities,

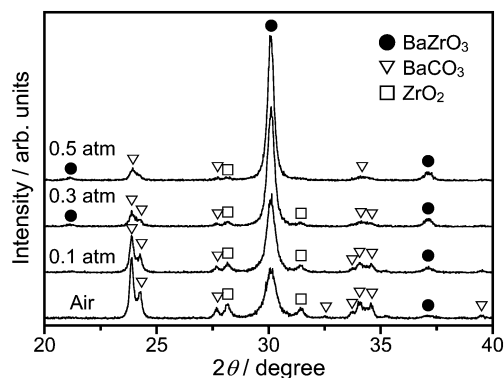


Fig. 4. XRD patterns of the products obtained by calcination at 900°C for 2 h in air and humid air with H₂O of 0.1–0.5 atm.

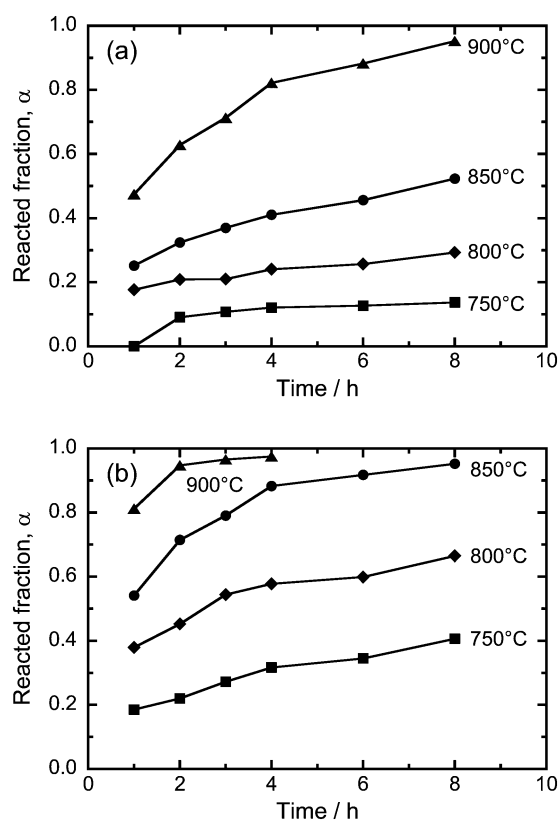


Fig. 5. Reaction kinetics of the BaCO₃-ZrO₂ mixture reacted in (a) air and (b) humid air with H₂O of 0.5 atm.

the reacted fraction of 63% was observed in air, whereas in humid air with H₂O of 0.5 atm the reacted fraction was 95%.

In order to elucidate the effect of water vapor on the solid-state formation of BaZrO₃ in the low temperature region, the reaction kinetics in air and humid air with H₂O of 0.5 atm was investigated at 750–900°C (before the second step for the BaZrO₃ formation as shown in Fig. 1). **Figure 5** shows the reacted fraction of the sample. In the case of the calcination in air [Fig. 5(a)], the formation ratios at 750 and 800°C did not change even the reaction time increased up to 8 h. At 850 and 900°C, the formation ratio was increased with increasing time. On the other hand, in the case of the calcination in humid air, the BaZrO₃ formation was accelerated even at 750°C. Comparing the formation ratios at 850°C in the both atmospheres, 1 h-calcination

in humid air was equivalent to 8 h-calcination in air. Therefore, the preparation of nanocrystalline BaZrO₃ powder in water vapor is completed at a lower temperature and in a shorter time than in air.

The reaction kinetics for the BaZrO₃ formation was analyzed by checking the agreement (the correlation coefficient, R^2) between the experimental data and the various kinetic model equations. We applied the kinetic model equations (three interface reaction models and four diffusion models) compiled by Koga and Criado²²⁾ to the experimental data. The interface reaction models assume that the reaction is controlled by the reaction interface progress toward the center of the reactant, whereas the diffusion models assume that diffusion of reactant or product is considered to be rate-controlling step. Depending on the particle shape, different mathematical models are derived.²³⁾ Only the data of α value under 0.9 was considered in the analysis. As a result, in the both atmospheres, the diffusion models were good correlation (mean R^2 of 0.962–0.972) rather than the interface reaction models (mean R^2 of 0.936–0.958). For the sample reacted in air, the two-dimensional diffusion (D2) model gives a better fit (mean R^2 of 0.969) and this equation is

$$\alpha + (1 - \alpha) \ln(1 - \alpha) = kt \quad (1)$$

where k is a kinetic constant and t the reaction time. The D2 model assumes that diffusion occurs radially through a cylindrical shell with an increasing reaction zone.²³⁾ On the other hand, in humid air, the three-dimensional diffusion (D3, Ginstling–Brounshtein) model,

$$1 - 2\alpha/3 - (1 - \alpha)^{2/3} = kt \quad (2)$$

is superior (mean R^2 of 0.972) to the D2 model (mean R^2 of 0.970). The D3 model is based on the assumption of a spherical particle reaction.²³⁾ However, there is not a significant difference in mean R^2 between D2 and D3 models for the reaction in humid air. Although the kinetic model for the BaZrO₃ formation previously reported by Ubaldini et al.¹¹⁾ is an interface reaction model at the ZrO₂–BaZrO₃ interface, the most likely rate-controlling step in this study is a diffusion process of ions. The difference between these results may be caused by the formation temperature. Under the experimental conditions in this study, BaZrO₃ is formed at a relatively low temperature. Therefore, the diffusion process of barium and oxygen ions into ZrO₂ particle are the most likely rate-controlling step. The apparent activation energy of the formation reaction was estimated by the Arrhenius equation:

$$k = A \exp(-E_a/RT) \quad (3)$$

where A is a constant, E_a the apparent activation energy, R the gas constant and T the absolute temperature. **Figure 6** shows the Arrhenius plot of $\ln k$ versus $1/T$ for D2 model in air and D3 model in humid air. From the slope of the liner curve in Fig. 6, the apparent activation energy for the BaZrO₃ formation was calculated to be 323 ± 21 kJ/mol and 263 ± 46 kJ/mol in air and humid air, respectively.

3.3 Accelerated solid-state synthesis in the 1 atm water vapor atmosphere

By increasing the water vapor partial pressure, the BaZrO₃ formation is accelerated, as shown in Fig. 4. We have previously reported the accelerated solid-state synthesis of the various double-oxide powders in the 1 atm water vapor atmosphere.^{12)–15)} Obviously, the BaZrO₃ formation in water vapor of 1 atm must proceed at a lower temperature than in air. **Figure 7** shows the

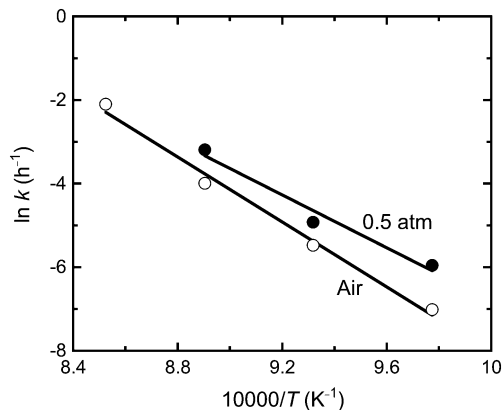


Fig. 6. Arrhenius plot of the kinetic constant for the BaZrO₃ formation in air and humid air with H₂O of 0.5 atm.

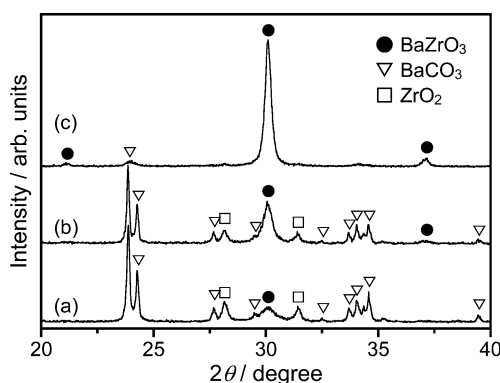


Fig. 7. XRD patterns of the products obtained by calcination at 750°C in (a) air for 12 h and water vapor of 1 atm for (b) 2 h and (c) 12 h.

XRD patterns for the products obtained by calcination at 750°C in air and water vapor of 1 atm. Even by calcination for 12 h in air, the product mainly consisted of BaCO₃ and ZrO₂ [Fig. 7(a)]. A trace amount of BaZrO₃ was formed by only the first step as shown in DTG curve (Fig. 1). In contrast, even for 2 h, the BaZrO₃ formation was accelerated in water vapor [Fig. 7(b)]. After calcination for 12 h in water vapor, the product exhibited almost single-phase BaZrO₃ [Fig. 7(c)]. Thus, water vapor clearly contributes to the low temperature synthesis of BaZrO₃.

3.4 The role of water vapor on the solid-state reaction

Water vapor promotes the decomposition of BaCO₃ at a lower temperature than its thermal decomposition temperature (>1000°C for pure BaCO₃^{11),20)}. The accelerated mechanism is due to the interaction between water vapor and BaCO₃ surface. For the thermal decomposition of CaCO₃, it has been reported that water vapor accelerates the decomposition of CaCO₃²⁴⁾ and weakens the Ca–CO₃ bond by surface adsorption.²⁵⁾ Surface reactivity is increased by the repetition of adsorption–desorption cycle of water molecules. In the case of the decomposition of BaCO₃, water vapor similarly might play an important role to weaken the Ba–CO₃ bond.

In addition, as pointed out in previously,^{11)–13)} a gas-phase transport of barium compounds is not negligible in the solid-state reaction in a water vapor atmosphere. It is reported that the volatility of BaO is greatly increased by the presence of water vapor because of the formation of volatile Ba(OH)₂ vapor.^{26),27)}

According to the thermodynamic data represented by L'vov,²⁸⁾ the vapor pressure of Ba(OH)₂ in the 1 atm water vapor atmosphere is calculated to be 9.2×10^{-6} atm at 800°C.¹³⁾ This value is 3–6 orders of magnitude higher than the other alkaline-earth hydroxides at the same temperature. Therefore, in the water vapor atmosphere, the contact areas between the reactants are increased by gas-phase transport, and then BaZrO₃ formation is promoted. As described above, the kinetic model for the BaZrO₃ formation in air and humid air was the two-dimensional and three-dimensional diffusion models, respectively. This result supports the suggestion that the formation reaction of BaZrO₃ in water vapor occurs at the entire ZrO₂ particle surface, whereas that in air proceeds only at the contact points between the reactants. Thus, water vapor can act as a catalyst in the solid-state reaction.

Comparing with the results of Ubaldini et al.,¹¹⁾ the results in this study have revealed the formation behavior of BaZrO₃ by in situ XRD measurement and the effect of water vapor at a lower temperature. Especially, it was shown that BaZrO₃ powder can be prepared in a water vapor atmosphere even at 750°C. By producing the 1 atm water vapor atmosphere, the effect of water vapor on the solid-state reaction was clearly observed. Under the high water vapor partial pressure, the decomposition of BaCO₃ and the gas-phase transport of barium compounds should occur from low temperature.

4. Conclusions

In this study, the solid-state reaction between very fine ZrO₂ (70 nm) and coarse BaCO₃ (1.5–5.7 μm) to form nanocrystalline BaZrO₃ powder (~80 nm) was investigated by DTG analysis and in situ XRD. The formation reaction of BaZrO₃ proceeded in two steps, which were located at 727 and 975°C from DTG analysis. The BaZrO₃ formation mainly occurred at the higher temperature (975°C) because of the thermal decomposition of BaCO₃. However, water vapor promoted the decomposition of BaCO₃ at a lower temperature than its thermal decomposition temperature. And then the BaZrO₃ formation was accelerated by increasing the water vapor partial pressure in the calcination atmosphere. The apparent activation energy for the BaZrO₃ formation decreased from 323 ± 21 kJ/mol in air to 263 ± 46 kJ/mol in humid air with H₂O of 0.5 atm. By calcination in the 1 atm water vapor atmosphere, the product at 750°C for 12 h exhibited almost single-phase BaZrO₃. The decomposition of BaCO₃ can be promoted by the interaction of BaCO₃ and BaO with water vapor. Water vapor-assisted solid-state reaction is effective technique to prepare double-oxide powders at a lower temperature and in a shorter time than the traditional method.

Acknowledgements This work was supported by Grant-in-Aid for JSPS Fellows (11J10693) and for Challenging Exploratory Research (24655195). The authors are also grateful to Dr. Tohru S. Suzuki of National Institute for Materials Science, Japan, for assistance with the SEM observation.

References

- 1) D. Segal, *J. Mater. Chem.*, **7**, 1297–1305 (1997).
- 2) D. F. K. Hennings, B. S. Schreinemacher and H. Schreinemacher, *J. Am. Ceram. Soc.*, **84**, 2777–2782 (2001).
- 3) M. T. Buscaglia, M. Bassoli, V. Buscaglia and R. Alessio, *J. Am. Ceram. Soc.*, **88**, 2374–2379 (2005).
- 4) S.-S. Ryu and D.-H. Yoon, *J. Mater. Sci.*, **42**, 7093–7099 (2007).
- 5) M. T. Buscaglia, M. Bassoli, V. Buscaglia and R. Vomberg, *J. Am. Ceram. Soc.*, **91**, 2862–2869 (2008).
- 6) R. Vassen, X. Cao, F. Tietz, D. Basu and D. Stöver, *J. Am. Ceram. Soc.*, **83**, 2023–2028 (2000).
- 7) T. Komatsu, O. Tanaka, C. Hirose, K. Matusita and T. Yamashita, *J. Mater. Sci. Lett.*, **9**, 170–172 (1990).
- 8) S. Kikkawa, F. Kanamaru and S. Hashiguchi, *J. Mater. Sci. Lett.*, **11**, 9–10 (1992).
- 9) J. L. Zhang and J. E. Evetts, *J. Mater. Sci.*, **29**, 778–785 (1994).
- 10) U. Anselmi-Tamburini, M. T. Buscaglia, M. Viviani, M. Bassoli, C. Bottino, V. Buscaglia, P. Nanni and Z. A. Munir, *J. Eur. Ceram. Soc.*, **26**, 2313–2318 (2006).
- 11) A. Ubaldini, V. Buscaglia, C. Uliana, G. Costa and M. Ferretti, *J. Am. Ceram. Soc.*, **86**, 19–25 (2003).
- 12) T. Kozawa, A. Onda and K. Yanagisawa, *J. Eur. Ceram. Soc.*, **29**, 3259–3264 (2009).
- 13) T. Kozawa, A. Onda and K. Yanagisawa, *J. Eur. Ceram. Soc.*, **30**, 3435–3443 (2010).
- 14) T. Kozawa, A. Onda and K. Yanagisawa, *Chem. Lett.*, **38**, 476–477 (2009).
- 15) T. Kozawa, K. Yanagisawa, A. Yoshida, A. Onda and Y. Suzuki, *J. Ceram. Soc. Japan*, **121**, 103–105 (2013).
- 16) T. Tatsuoka and N. Koga, *J. Am. Ceram. Soc.*, **95**, 557–564 (2012).
- 17) V. Ischenko, E. Pippel, R. Köferstein, H.-P. Abicht and J. Woltersdorf, *Solid State Sci.*, **9**, 21–26 (2007).
- 18) V. Ischenko, J. Woltersdorf, E. Pippel, R. Köferstein and H.-P. Abicht, *Solid State Sci.*, **9**, 303–309 (2007).
- 19) K. Tsuzuku and M. Couzi, *J. Mater. Sci.*, **47**, 4481–4487 (2012).
- 20) I. Arvantidis, Du. Sichen and S. Seetharaman, *Metall. Mater. Trans., B, Process Metall. Mater. Proc. Sci.*, **27**, 409–416 (1996).
- 21) J. O. A. Paschol, H. Kleykamp and F. Thümmel, *J. Nucl. Mater.*, **151**, 10–21 (1987).
- 22) N. Koga and J. M. Criado, *J. Am. Ceram. Soc.*, **81**, 2901–2909 (1998).
- 23) A. Khawam and D. R. Flanagan, *J. Phys. Chem. B*, **110**, 17315–17328 (2006).
- 24) W. H. MacIntire and T. B. Stansel, *Ind. Eng. Chem.*, **45**, 1548–1555 (1953).
- 25) Y. Wang and W. J. Thomson, *Chem. Eng. Sci.*, **50**, 1373–1382 (1995).
- 26) F. E. Stafford and J. Berkowits, *J. Ceram. Phys.*, **40**, 2963–2969 (1964).
- 27) T. Sasamoto, K. Mizushima and T. Sata, *Bull. Chem. Soc. Jpn.*, **52**, 2127–2129 (1979).
- 28) B. V. L'vov, *Thermochim. Acta*, **303**, 161–170 (1997).